IMPROVEMENTS TO AUTOMATED BEAM-SIZE MEASUREMENT SYSTEM AT KEKB

J.W. Flanagan, S. Hiramatsu, H. Ikeda, T. Mitsuhashi, KEK, Tsukuba, Ibaraki, Japan

Abstract

In order to measure beam sizes at KEKB, we have installed synchrotron radiation (SR) monitors in each of the electron and positron storage rings, capable of both direct imaging and SR interferometry measurements. The interference pattern from the SR interferometer is digitized and analyzed automatically for continuous beam-size measurements in both the horizontal and vertical transverse planes, which are used for beam-size studies and also during normal running for luminosity optimization. We here report on recent improvements for stabilization and reduction of systematic errors in the system.

1 INTRODUCTION

Two sets of SR interferometers are installed at the KEKB B-Factory, one set at each ring.[1] In each ring, the light is generated at a 5 mrad bending magnet ("weak bend") and is extracted from the ring by a water-cooled beryllium mirror. Over the course of operation, systematic problems associated with the heating of the mirrors have shown up at high beam currents. One problem is that the optical axis moves out of alignment with beam current. Another serious problem is a change of apparent beam size with beam current. These problems and their practical solutions are discussed here.

2 OPTICAL AXIS STABILIZATION

As the beam intensity changes and the mirror heats up, the mirror tends to pivot around its mounting points, changing the orientation of the face. This change in mirror angle causes the angle of the optical axis to change by amounts on the order of 1 mrad, which when propagated down the 30 m path to the optics hut leads to an unacceptably large shift in the position of the light impinging on the interferometer slits. To correct for this shift, we monitor the central position of the interference patterns on the camera face, and adjust the orientation of a remotely-movable mirror which is located just outside the beam pipe, 35 cm downstream of the extraction mirror.

The optical axis feedback operates continuously on a 10-second cycle. Typical feedback compensation angles (the inverse of the mirror angle) are shown in Figure 2 for the LER mirror over the course of several fills from a cold start. As can be seen, the vertical

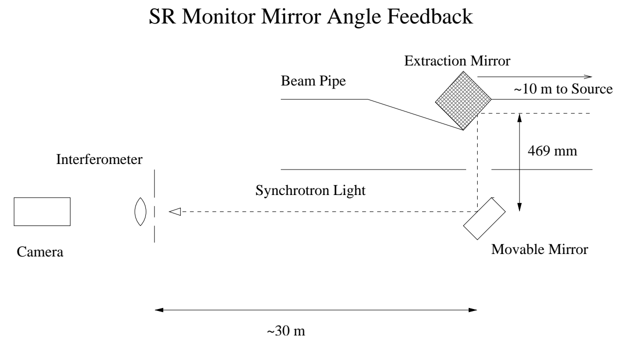

Figure 1: Optical axis feedback.

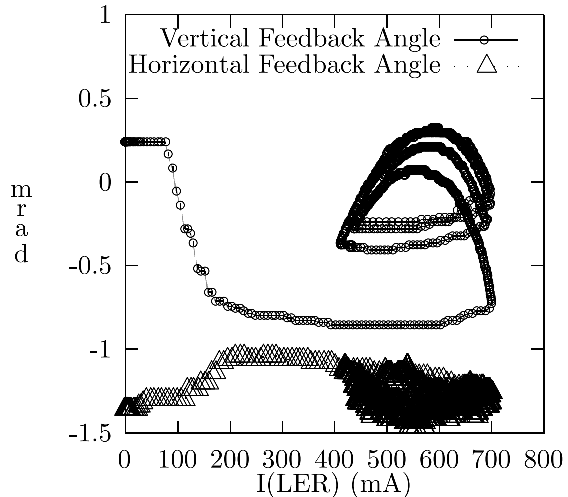

Figure 2: Mirror feedback history from cold start through several fills.

angle motion spans over 1 mrad for the vertical axis, and about 0.5 mrad for the horizontal axis. Significant hysteresis is also present: after injection is stopped at 700 mA (in this case), the maximum deviation is not reached until the beam current decays to 550-600 mA, some 30 minutes later. Optical axis feedback is employed for both the LER and HER mirrors.

3 APPARENT BEAM SIZE

In the treatment that we have previously used for analyzing interferograms, the interferogram for a single-wavelength λ of the incident SR from double slits of width w and separation D has an intensity distribution $y(x)$ of the form[2],

$$y(x) = I_0 \left[\frac{sin(\frac{2\pi}{\lambda}\frac{w}{F}x)}{\frac{2\pi}{\lambda}\frac{w}{F}x} \right]^2 (1 + \gamma cos(\frac{2\pi}{\lambda}Dx)), \qquad (1)$$

where I_0 is the intensity of the light reaching each slit assuming the intensities I_1 and I_2 at each slit are equal ($I_1 = I_2 \equiv I_0$). This represents two single-slit diffraction patterns $(sin(x)/x)^2$ brought into overlap by a lens behind the slits onto a CCD imaging plane at a distance F from the lens, modulated by a cosine double-slit term with visibility γ determined by the spatial coherence of the SR light. The beam size is calculated from the visibility as,

$$\sigma_{beam} = \frac{\lambda L}{\pi D}\sqrt{\frac{1}{2}\ln\frac{1}{\gamma}}, \qquad (2)$$

where L is the distance from the SR source point to the slits and the beam distribution is assumed to be Gaussian.

Now, as the beam current increases the temperature of the beryllium extraction mirror rises, causing a deformation of the mirror surface as the mirror block expands. The resulting curvature changes the propagation angles of the light rays which pass the interferometer slits, causing a change in the apparent beam size which can be quite severe (30%).

The see how this happens, see Figure 3. The heat-deformed mirror surface is shown as a solid black line, as are the light paths from the SR source point to the interferometer slits. The ideal (undeformed) mirror surface and its corresponding light paths are shown as dashed lines. Immediately downstream of the extraction mirror is a dotted line representing a plane where a pinhole mask (see below) for measuring mirror distortion is located. The light rays which reach the interferometer slits depart from the source at an angular divergence of $\theta = D/L$. The distance between the light rays at the mask plane (at distance $L\prime$) is $D\prime$. If the distance from the extraction mirror to the mask plane is much smaller than the distance from the source to the mask plane, and for small angular divergences, $\theta \approx D\prime/L\prime$.

If the mirror is undeformed, then $D\prime = D_0\prime$, where $D_0\prime/L\prime = D/L = \theta_0$. Thus, equation 2 can be expressed as

$$\sigma_{beam} = \frac{\lambda}{\pi\theta_0}\sqrt{\frac{1}{2}\ln\frac{1}{\gamma}} = \frac{\lambda L\prime}{\pi D_0\prime}\sqrt{\frac{1}{2}\ln\frac{1}{\gamma}}. \qquad (3)$$

However, in the case of a deformed mirror, $\theta \neq \theta_0$ and $D\prime/L\prime \neq D/L$. In this case, it is necessary to

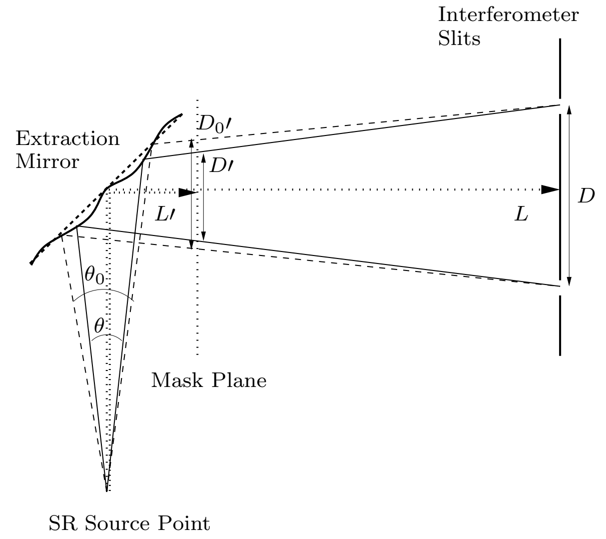

Figure 3: Effect of mirror distortion on ray propagation.

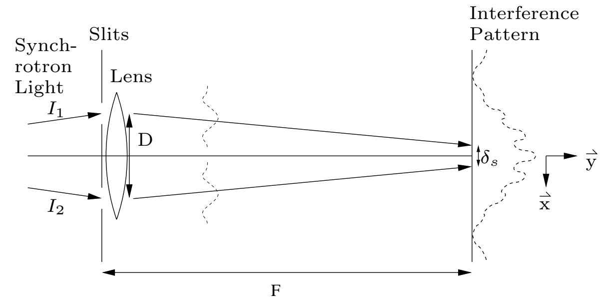

Figure 4: Interference pattern formation.

determine $D\prime$ ($L\prime$ never changes) in order to make the correct estimate of the beam size:

$$\sigma_{beam} = \frac{\lambda}{\pi\theta}\sqrt{\frac{1}{2}\ln\frac{1}{\gamma}} = \frac{\lambda L\prime}{\pi D\prime}\sqrt{\frac{1}{2}\ln\frac{1}{\gamma}}. \qquad (4)$$

One method of determining $D\prime$ is to use a Hartmann pinhole mask.[3] By moving a pinhole mask across the mask plane, the spots on the mask plane from which light rays propagate to the interferometer slit positions can be easily located (they are the locations at which one or the other slit is illuminated by the SR light which has passed through the pinhole), and $D\prime$ can be measured.

However, this method is very time-consuming and is not usable in normal operation, since the interferometer cannot be used when the mask is in place due to one slit being always blocked. Also, given the large thermal hysteresis mentioned in the previous section, it is not possible to simply measure the distortion curve once and apply a correction factor as a function of beam current, as the beam current history plays a role. For this reason we have developed a method

for measuring and correcting for this distortion during real-time operation of the interferometer based on modifying the fitting procedure used to analyze the interference pattern visible after the slits.

4 NEW FITTING PROCEDURE

In order to find D', we now fit the interference pattern to an equation of the form

$$y(x) = a + bx + \frac{m}{2}\sum_i t_i \times$$
$$\left\{ A_1^2 + A_2^2 + 2A_1A_2\gamma^{\left(\frac{\lambda_0}{\lambda_i}\right)^2} \cos\left[\beta_c\left(\frac{\lambda_0}{\lambda_i}\right)(x-\phi_c)\right]\right\},$$

where

$$A_1 = \sqrt{1+\alpha_I}\,\frac{\sin\left[\beta_s(1+\alpha_s)\left(\frac{\lambda_0}{\lambda_i}\right)\left(x-\left(\phi_s-\frac{\delta_s}{2}\right)\right)\right]}{\beta_s(1+\alpha_s)\left(\frac{\lambda_0}{\lambda_i}\right)\left(x-\left(\phi_s-\frac{\delta_s}{2}\right)\right)},$$

$$A_2 = \sqrt{1-\alpha_I}\,\frac{\sin\left[\beta_s(1-\alpha_s)\left(\frac{\lambda_0}{\lambda_i}\right)\left(x-\left(\phi_s+\frac{\delta_s}{2}\right)\right)\right]}{\beta_s(1-\alpha_s)\left(\frac{\lambda_0}{\lambda_i}\right)\left(x-\left(\phi_s+\frac{\delta_s}{2}\right)\right)},$$

and t_i is the transmission at wavelength λ_i of the band-pass filter with central wavelength λ_0.

In this fit, the two single-slit diffraction terms are represented by A_1 and A_2, wherein α_I represents the asymmetry $\frac{I_1-I_2}{I_1+I_2}$ of the light intensities I_1 and I_2 impinging on the two slits. $\beta_s(1\pm\alpha_s)$ represent the widths of the single-slit *sinc* terms from each slit, with α_s representing the (usually very small) asymmetry between the widths of the patterns from each slit. $\phi_s \pm \frac{\delta_s}{2}$ represent the centers of the single-slit terms, separated by δ_s from each other.

Changes in δ_s are correlated with deformations in the mirror. The reason for this is that as D' after the mirror changes, the angle between the rays reaching the slits changes. This in turn causes the angles between the rays after the lens to change. Since the surface of the camera CCD remains at a fixed distance (F) from the slits/lens, the centers of the single-slit terms A_1 and A_2 move relative to each other on the CCD surface. (See Fig. 4.) By measuring the change in δ_s the deformation can be monitored and corrected for in real-time during interferometer usage.

For small values of δ_s relative to the longitudinal coherence depth, the relationship between D' and δ_s should be approximately linear. We took calibration data over the full range of beam currents in use, and plotted the effective slit separation at the mask plane D', as measured using the pinhole mask, versus δ_s. The data are shown in Figure 5. The standard deviation to a linear fit is less than one percent, verifying that δ_s can be used to estimate D' without needing to use the pinhole mask after initial calibration.

The fit procedure previously used[4] can be derived from the current one by holding δ_s, α_I and α_s at zero.

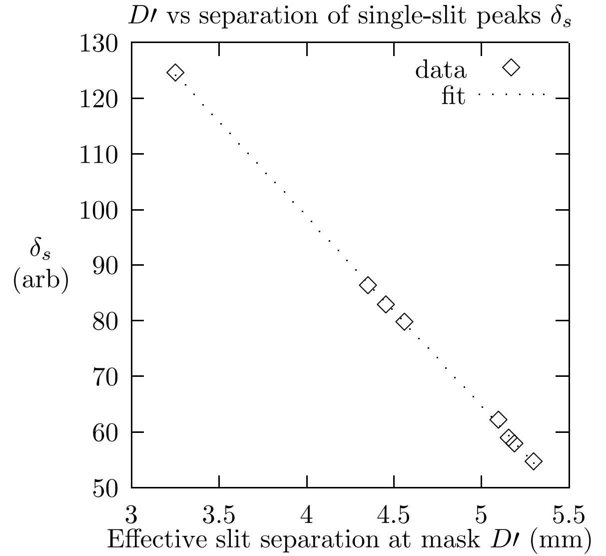

Figure 5: D' vs δ_s

The most important term for correction of apparent beam size is the inclusion of the δ_s term. The light intensity asymmetry parameter α_I corrects for the secondary effects of changes in the light distribution due to mirror distortion.

Tests of the system in the Spring of 2001 on the vertical interferometer of the KEKB LER indicate that the method works well. Extension to the LER horizontal, and HER vertical and horizontal interferometers is planned next.

5 ACKNOWLEDGMENTS

The authors wish to thank Professors S. Kurokawa and K. Oide for their encouragement of this work. The authors also thank the KEKB commissioning team for their support and feedback.

6 REFERENCES

[1] T. Mitsuhashi, J.W. Flanagan, S. Hiramatsu, "Optical Diagnostic System for the KEK B-Factory," Proceedings of EPAC 2000, Vienna, Austria, p. 1783

[2] T.Mitsuhashi, "Beam Profile and Size Measurement by SR Interferometers," Proceedings of 1998 Joint US-CERN-Japan-Russia School on Particle Accelerators (Beam Measurement), Montreux and CERN, Switzerland (1998) pp. 399-427

[3] D. Malacara, ed., Optical Shop Testing, Second edition, Wiley (New York) 1992, pp. 367-396.

[4] J.W. Flanagan, S. Hiramatsu, T. Mitsuhashi, "Automatic Continuous Transverse Beam-size Measurement System for KEKB," Proceedings of EPAC 2000, Vienna, Austria, p. 1714